H^+/solute-induced intracellular acidification leads to selective activation of apical Na^+/H^+ exchange in human intestinal epithelial cells

David T. Thwaites, Dianne Ford, Michael Glanville, and Nicholas L. Simmons

Department of Physiological Sciences, Medical School, University of Newcastle upon Tyne, Newcastle upon Tyne NE2 4HH, United Kingdom

Address correspondence to: D.T. Thwaites, Department of Physiological Sciences, Medical School, University of Newcastle upon Tyne, Newcastle upon Tyne NE2 4HH, United Kingdom. Phone: 44-191-222-8559; Fax: 44-191-222-6706; E-mail: d.t.thwaites@ncl.ac.uk.

Received for publication April 27, 1999, and accepted in revised form July 13, 1999.

The intestinal absorption of many nutrients and drug molecules is mediated by ion-driven transport mechanisms in the intestinal enterocyte plasma membrane. Clearly, the establishment and maintenance of the driving forces — transepithelial ion gradients — are vital for maximum nutrient absorption. The purpose of this study was to determine the nature of intracellular pH (pH_i) regulation in response to H^+-coupled transport at the apical membrane of human intestinal epithelial Caco-2 cells. Using isoform-specific primers, mRNA transcripts of the Na^+/H^+ exchangers NHE1, NHE2, and NHE3 were detected by RT-PCR, and identities were confirmed by sequencing. The functional profile of Na^+/H^+ exchange was determined by a combination of pH_i, $^{22}Na^+$ influx, and EIPA inhibition experiments. Functional NHE1 and NHE3 activities were identified at the basolateral and apical membranes, respectively. H^+/solute-induced acidification (using glycylsarcosine or β-alanine) led to Na^+-dependent, EIPA-inhibitable pH_i recovery or EIPA-inhibitable $^{22}Na^+$ influx at the apical membrane only. Selective activation of apical (but not basolateral) Na^+/H^+ exchange by H^+/solute cotransport demonstrates that coordinated activity of H^+/solute symport with apical Na^+/H^+ exchange optimizes the efficient absorption of nutrients and Na^+, while maintaining pH_i and the ion gradients involved in driving transport.

J. Clin. Invest. **104**:629–635 (1999).

Introduction

H^+-coupled transport of protein-digestion products (di- and tripeptides), orally absorbed drugs (e.g., some aminocephalosporin antibiotics and the angiotensin-converting enzyme inhibitors enalapril and captopril), and sugars has been demonstrated in a number of studies (1–6). Our own studies demonstrate that the transport and cellular accumulation of certain amino acids (such as the osmoregulatory β-amino acids taurine and β-alanine, and the orally absorbed antibiotic D-cycloserine) across the apical membrane of human intestinal epithelial cells is energized by extracellular acidification. This amino acid transport is coupled with proton inflow in monolayers of Caco-2 cells that have been loaded with the pH-sensitive fluorescent dye BCECF (BCECF; refs. 7, 8). These observations emphasize the potential importance of the H^+ electrochemical gradient as a driving force of solute absorption across the mammalian intestinal wall. Clearly, the development and maintenance of such driving forces (transepithelial and transmembrane ion gradients) during nutrient transport are crucial for efficient absorption. Local microdomains of pH exist within the unstirred layers adjacent to intestinal surfaces (in the intervillus and lateral spaces; refs. 9–11). Indeed, an acid microclimate has been demonstrated at the apical membrane both in vivo and in vitro (9, 10), suggesting that a chemical driving force for H^+ exists across the brush border of the intestinal epithelium. Ion-driven absorption is thus controlled by the ion composition within the microdomain, suggesting that absorptive capacity can be regulated. Such pH microdomains are subject to physiological and pathophysiological regulation, as is observed with short-chain fatty acids (11, 12) and enterotoxins (9).

Therefore, H^+ transport across the intestinal brush border membrane is not a simple leak flux, but is coupled to perform useful work in accumulating substrates such as di- and tripeptides and amino acids. The capacity of H^+/substrate symport (relative to Na^+/substrate symport) is unknown, although our own data suggest that it is the predominant route for some amino acids (13). However, this solute-induced H^+ influx will place a significant acid load on intracellular pH (pH_i) and pH-homeostatic mechanisms.

In many cell types, regulation of pH_i is carried out by a family of Na^+/H^+ exchangers (NHEs) that exchange Na^+ and H^+ ions at the plasma membrane (14–17). NHE1 has a ubiquitous distribution, but is restricted to the basolateral plasma membrane in both intestinal and renal epithelia. In contrast, NHE3 is present only at the apical membrane in intestinal and renal

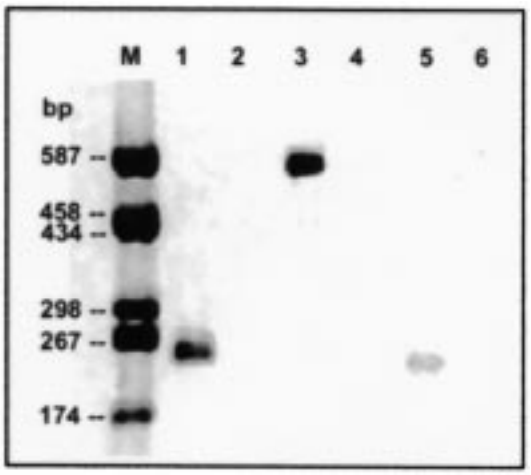

Figure 1
Products of RT-PCR on Caco-2 poly(A)$^+$ RNA using primers specific for *NHE1* (lanes 1 and 2), *NHE2* (lanes 3 and 4), and *NHE3* (lanes 5 and 6). Lane M shows DNA markers with sizes indicated. Lanes 2, 4, and 6 show negative-control reactions, carried out in the absence of MMLV-RT. Products were separated on a 1% agarose gel and stained with ethidium bromide. Primer sequences and thermal cycling parameters are given in Methods.

epithelial cells (16, 17). An important feature of Na^+/H^+ exchange is that the exchanger(s) is quiescent, or is operating at only a very small fraction of its potential maximum capacity, at the (neutral) pH values typical of cytosol (14). Indeed, characterization of NHE activity often involves recovery from acid load after NH_4Cl prepulse.

After a meal, the intestinal lumen contains a mixed complement of substrates, such as di- and tripeptides, amino acids, and sugars. The total magnitude of transepithelial Na^+ transport mediated by Na^+/H^+ exchange in these conditions is unclear, although ileal Na^+ and water absorption are blocked by *N,N*-dimethylamiloride at concentrations consistent with NHE2 and NHE3 activity (18). We asked whether apical NHE activity can maintain sufficient Na^+ entry for transepithelial Na^+ transport to occur while apparently operating at a low rate relative to its maximum capacity.

In this study, we have used Caco-2 cell monolayers grown on permeable filters as a model to represent the human small intestinal epithelium. There were 2 primary objectives: to demonstrate the mutual functional expression of Na^+/H^+ exchange, H^+/dipeptide transporters, and H^+/amino acid transporters; and to test the hypothesis that dissipative H^+/solute influx provides an indirect means by which apical Na^+/H^+ exchange is stimulated. Such stimulation would ensure maintenance of the ion gradients and pH microclimate required to drive H^+/solute symport. It is likely that the coordinated operation of discrete membrane transporters is required to explain overall function at the brush border of the human small intestine. Although a relationship between H^+/peptide exchange and Na^+/H^+ exchange has been hypothesized, little direct evidence is currently available. Because modulation of Na^+/H^+ activity is associated with changes in the acid microclimate, and therefore with the H^+ electrochemical gradient across the apical membrane of the small intestinal epithelium, it is likely that during pathophysiological regulation (e.g., after pathogenic invasion by *Escherichia coli*; ref. 9) any transport function that is dependent on the maintenance of the ion gradients across the epithelium will also be affected. The identification of a functional linkage between H^+/solute transport and pH_i homeostasis demonstrates the coordinated nature of absorption, and highlights the potential risk of studying individual transport proteins in isolation.

Methods

Materials. ^{22}NaCl (specific activity: ~17 GBq/mg Na) was from Amersham Life Science Products Ltd. (Little Chalfont, Buckinghamshire, United Kingdom). β-alanine, glycylsarcosine (Gly-Sar), ouabain, cell culture media, and supplements were from Sigma-Aldrich Ltd. (Poole, Dorset, United Kingdom). BCECF-AM was from Calbiochem-Novabiochem Ltd. (Nottingham, United Kingdom). Cell culture plasticware was from Corning-Costar Ltd. (High Wycombe, United Kingdom). EIPA was from RBI (Natick, Massachusetts, USA). All other chemicals were from Merck (BDH) Ltd. (Poole, Dorset, United Kingdom) and were of the highest quality available.

Cell culture. Caco-2 cells (passage number 98–126) were cultured and prepared as monolayers as described previously (5). Experiments were performed 15–21 days after seeding, and 18–24 hours after feeding.

RT-PCR. Poly(A)+ RNA was prepared from Caco-2 cells grown under standard conditions for 21 days. The method for poly(A)+ RNA isolation (based on detergent lysis, digestion of RNases with proteinase K, and capture of polyadenylated molecules on oligo-dT cellulose) has been described previously (19). Poly(A)+ RNA was reverse transcribed using Moloney murine leukemia virus reverse transcriptase (MMLV-RT; MBI Fermentas Inc., Amherst, New York, USA) and random hexanucleotide primers (Amersham Pharmacia Biotech Ltd., Albans, United Kingdom) in a standard reaction. PCR was carried out using primers for NHE1 and NHE2 as described by Dudeja et al. (20), and for NHE3 based on the published human sequence (21). Note that the NHE2 primers were designed for the human intestinal NHE2 fragment (20) and not the longer NHE2 sequence identified from human liver (22). The primers used were as follows:

NHE1: $_{336}$GACTACACACACGTGCGCACCCC$_{348}$
$_{568}$TCCAGGATGATGGGCGGCAGCAGGAAGAGGAA$_{537}$
NHE2: $_{16}$GAAGATGTTTGTGGACATTGGGG$_{38}$
$_{565}$CGTCTGAGCTGCTGCTATTGC$_{545}$
NHE3: $_{2070}$AGAAGCGGAGAAACAGCAG$_{2088}$
$_{2286}$GGAGAAAACACAGGGTTGTC$_{2267}$

PCR reactions were performed over 30 cycles (after hot start) in 1.5 mM $MgCl_2$ using recombinant *Taq* polymerase (MBI Fermentas Inc.) in the manufacturer's buffer. Thermal cycling parameters were as follows:

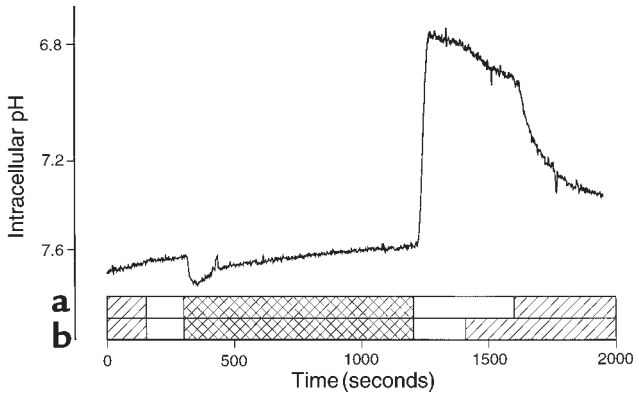

Figure 2
Identification of Na^+/H^+ exchange activity in Caco-2 cell monolayers. NH_4Cl-induced intracellular acidification in monolayers of Caco-2 cells. pH_i was measured in monolayers of Caco-2 cells loaded with the pH-sensitive fluorochrome BCECF. The solutions (all pH 7.4) bathing both the apical (**a**) and basolateral (**b**) membranes were standard Na^+-containing Krebs-Ringer (hatched bars), Na^+-free Krebs-Ringer (open bars), and Na^+-free Krebs-Ringer containing NH_4Cl (cross-hatched bars). Cells were exposed to 30 mM NH_4Cl for 15 minutes; NH_4Cl was removed in Na^+-free conditions followed by sequential addition of Na^+ to the basolateral and then apical solutions.

for *NHE1* and *NHE2*, 94°C for 1 minute, 58°C for 1 minute, and 72°C for 2 minutes; for *NHE3*, 94°C for 1 minute, 55°C for 1 minute, and 72°C for 2 minutes. Products were subcloned into the vector pUAG (Ingenius, R and D System Ltd., Abingdon, United Kingdom) or PCR2.1-TOPO (Invitrogen Corp., San Diego, California, USA) and sequenced on an ABI Prism model 377 automated sequencer (Perkin-Elmer Applied Biosystems, Warrington, United Kingdom).

The *NHE2* sequence contained differences from the published sequences. To determine whether the differences represented *Taq*-induced nucleotide misincorporation, the PCR was repeated using the thermostable proofreading enzyme *Pwo* polymerase (Boehringer Mannheim GmbH, Mannheim, Germany). Thermal cycling parameters were as follows: 10 cycles at 94°C for 15 seconds, 56°C for 30 seconds, and 72°C for 45 seconds; 20 cycles at 94°C for 15 seconds, 54°C for 30 seconds, and 72°C for 45 + 20 seconds per cycle; and then a 10-minute incubation at 72°C including *Taq* DNA polymerase (MBI Fermentas Inc.) to incorporate A-overhangs for TA cloning into the pCR2.1-TOPO vector (Invitrogen Corp., San Diego, California, USA). Clones were sequenced as above.

Experimental solutions. The transport and pH_i experiments were performed using a standard Krebs-Ringer solution containing (in mmol/L) 137 NaCl, 5.4 KCl, 2.8 $CaCl_2$, 1.0 $MgSO_4$, 0.3 NaH_2PO_4, 0.3 KH_2PO_4, 10 glucose, and 10 HEPES or MES (pH was adjusted to 7.4 or 5.5 at 37°C with Tris base). Na^+-free Krebs-Ringer solution was prepared by replacing NaCl with equimolar choline chloride and omitting NaH_2PO_4. An NH_4Cl-containing solution was identical to the Na^+-free solution except that 30 mM NH_4Cl replaced 30 mM choline chloride. Substrate additions were made directly to the Krebs-Ringers (e.g., 20 mM Gly-Sar or 20 mM β-alanine). Control solutions contained 20 mM mannitol to maintain equivalent osmotic strength.

Transport experiments. For uptake experiments, the cell monolayers (grown on 12-mm-diameter filters) were extensively washed 4 times by successive transfer through beakers containing 500 mL of Na^+-free Krebs-Ringer, and placed in 12-well plates, with each well containing 1 mL of prewarmed Na^+-free Krebs-Ringer (pH 7.4). Aliquots (0.5 mL) of prewarmed Na^+-free Krebs-Ringer (pH 7.4) were then placed in the upper filter cup (apical solution). The composition of the solutions in the apical and basal chambers was identical except when stated otherwise. For experiments requiring a preincubation period, cell monolayers were incubated for 15 minutes at 37°C in an appropriate Na^+-free Krebs-Ringer solution (see figure legends for details). After preincubation, filters were removed from the 12-well plates and washed in 500 mL of Na^+-free Krebs buffer (37°C). For uptake measurements, filters were then placed in a fresh 12-well plate containing 1 mL prewarmed Na^+-free buffer (pH 7.4) containing 1 mM ouabain. Aliquots (0.5 mL) of prewarmed Na^+-free Krebs buffer (pH 7.4) were added to the apical chamber. ^{22}Na (1 μCi/mL) was added to either the apical or basal solution, and uptake was measured over a 5-minute period. At the end of the incubation period, cell monolayers were washed 4 times in 500-mL volumes of ice-cold Na^+-free Krebs buffer (pH 7.4) to remove any loosely associated radiolabel, and were removed from the insert. Cell monolayer–associated radiolabel was determined by scintillation counting. Cellular uptake of substrates is expressed as fmol•cm^{-2}.

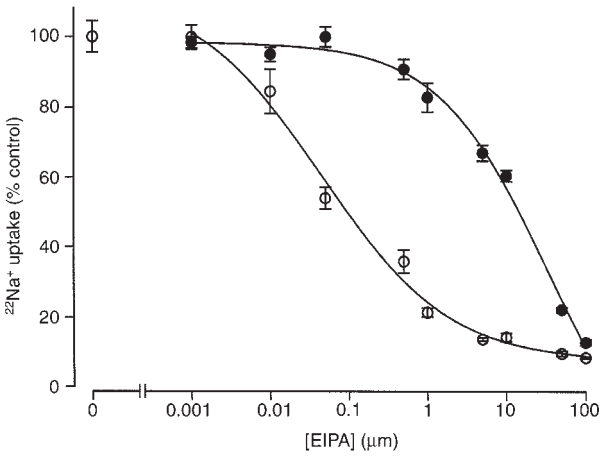

Figure 3
Identification of Na^+/H^+ exchange activity in Caco-2 cell monolayers. Shown is dose-dependent EIPA inhibition of $^{22}Na^+$ influx across apical (filled circles) and basolateral (open circles) membranes of Caco-2 cell monolayers after a 15-minute incubation with 30 mM NH_4Cl. Solid lines are the best-fit curves for a logistic sigmoid by least-squares regression (FigP software; biosoft, Cambridge, United Kingdom). Results are mean ± SEM (n = 6).

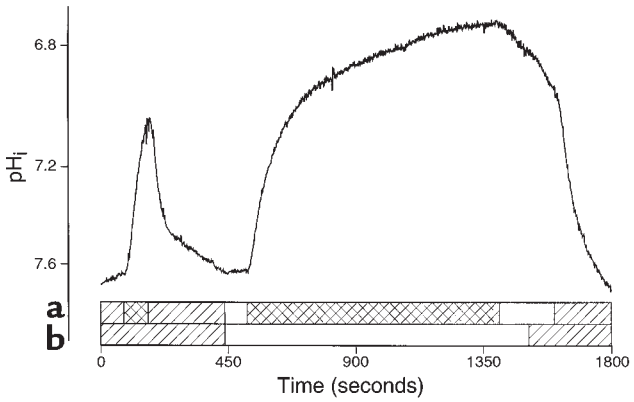

Figure 4
Solute-induced Na^+/H^+ exchange activity in Caco-2 cell monolayers. The effects on pH_i of altering the bathing solution at either the apical (**a**) or basolateral (**b**) membrane of Caco-2 cell monolayers. The solutions (see Methods) were Na^+-containing, pH 7.4 (hatched bars); Na^+-free, pH 7.4 (open bars); and Na^+-free, pH 5.5, containing β-alanine (20 mM; cross-hatched bars). Note that β-alanine was added to the apical surface only.

Measurement of pH_i. Measurements of pH_i in Caco-2 cells (grown to confluence on 12-mm-diameter Transwell polycarbonate filters) were performed essentially as described previously (5). To calculate the relative H^+ efflux rate in the presence or absence of extracellular Na^+, the rate of recovery was determined by linear regression (using Photon Counter System 4.70 software; Newcastle Photometric Systems, Newcastle upon Tyne, United Kingdom) of the pH_i recovery trace over a 30-second period immediately before, and another 30-second period immediately after, each change in solution. Because differences in linear rates of pH_i change are compared on either side of the experimental change, buffering capacities in these conditions will be equal. Recoveries of pH were measured at approximately pH 6.8–7.0, where buffering capacity is 18–19 mM/pH unit (23). Buffering capacity combined with the rate of pH_i change ($\Delta pH_i/s$) allows calculation of H^+ efflux rates (μM/s; ref. 24).

Statistics. Results are expressed as mean ± SEM. Statistical comparison of mean values were made using 1-way ANOVA, with a corrected Bonferroni *P* value for the number of comparisons made.

Results

Identification of NHEs in Caco-2 cells. Expression of NHE isoforms in Caco-2 cells was determined using a combination of molecular and cellular biological techniques (RT-PCR, $^{22}Na^+$ influx, and measurement of pH_i). Oligonucleotide primers specific to the published human *NHE1* (25), *NHE2* (20), and *NHE3* (21) sequences (see Methods) were designed and used for RT-PCR analysis of poly(A)$^+$ RNA, which was prepared from Caco-2 cell monolayers 21 days after seeding. The primer pairs produced PCR products of the predicted sizes (233 bp, 550 bp, and 217 bp for *NHE1*, *NHE2*, and *NHE3*, respectively; Figure 1). PCR products were subcloned into either pUAG or pCR2.1-TOPO (see Methods) and sequenced, showing 100% (*NHE1* and *NHE3*) and 99% (to intestinal *NHE2*; 82% to liver *NHE2*) identity to the published human sequences over the amplified regions. The nucleotide changes in the *NHE2* sequence were confirmed by PCR using a high-fidelity enzyme; 3 clones had identical sequences in both strands. The PCR products aligned with nucleotides 336–568 of the human *NHE1* sequence (25), nucleotides 16–565 of the human intestinal *NHE2* sequence (20) (nucleotides 1619–2168 of the human liver *NHE2*; ref. 22), and nucleotides 2070–2286 of the human *NHE3* sequence (21). The *NHE3* sequence was an exact match to the published sequence except for a missing cytosine at position 2177. This must represent an error in the published sequence, because translation of the published sequence causes frameshift after this point, with premature stop codons.

Confirmation of cellular expression and localization of NHE activity was made by measurement of pH_i and $^{22}Na^+$ influx. NH_4Cl prepulse (30 mM, 15 minutes) and release caused a marked intracellular acidification of BCECF-loaded Caco-2 cells, with recovery dependent on the presence of Na^+ at both the apical and basolateral membranes (Figure 2). $^{22}Na^+$ influx (linear up to 5 minutes) was significantly increased across both apical (70.1 ± 7.0 to 266.7 ± 15.3 fmol•cm^{-2}) and basolateral (27.8 ± 1.2 to 156.9 ± 17.1 fmol•cm^{-2}; for all measurements, n = 21 and P < 0.001) membranes after the NH_4Cl prepulse-and-release maneuver, and was EIPA-sensitive (half-maximal inhibition at 10 μM and 46 nM for apical and basal uptake, respectively; Figure 3).

Selective activation of apical NHE. In contrast to the response after NH_4Cl exposure, intracellular acidification caused by H^+/solute (dipeptide or amino acid) sym-

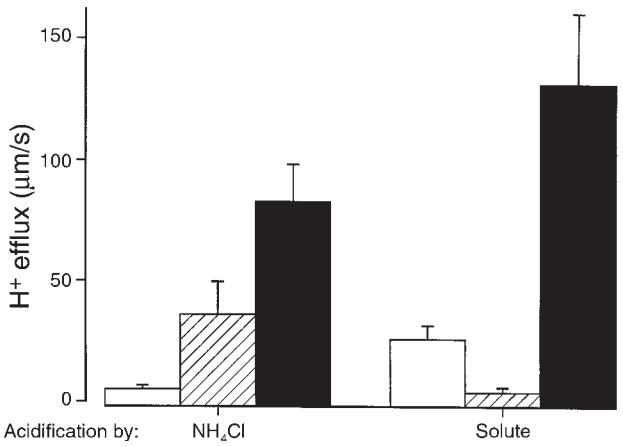

Figure 5
Solute-induced Na^+/H^+ exchange activity in Caco-2 cell monolayers. Mean H^+ efflux rates after incubation with either 30 mM NH_4Cl (n = 5) or 20 mM solute (dipeptide or amino acid; n = 13). The values represent the recovery from intracellular acidification in Na^+-free conditions (open bars), the increase in rate of recovery upon addition of basal Na^+ (hatched bars), and the further increase upon addition of apical Na^+ (solid bars). Results are mean ± SEM.

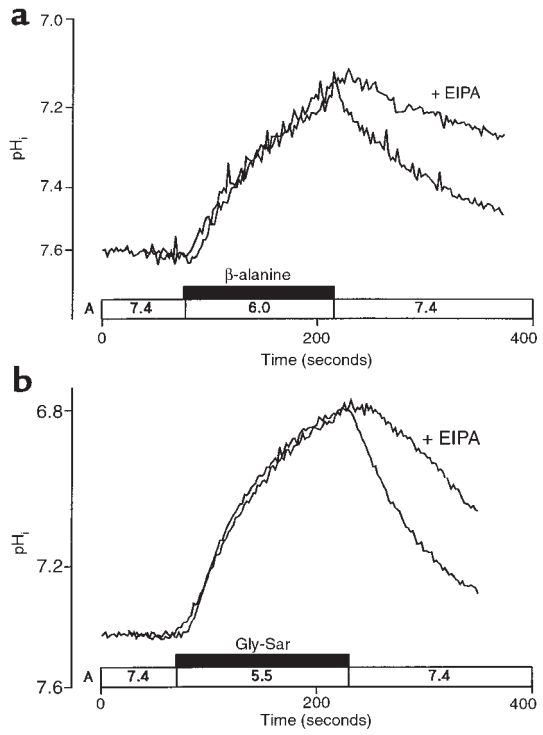

Figure 6
Effect of apical EIPA (100 μM) on Na^+-dependent pH_i recovery after acidification with 20 mM of either β-alanine (**a**) or Gly-Sar (**b**) in Na^+-containing solutions. The composition and pH of the apical solution is indicated by the horizontal bar. Basolateral pH was maintained at 7.4. The trace represents the composite response seen in a single monolayer to successive recoveries in the absence and presence of EIPA.

port across the apical membrane stimulates apical, but not basolateral, Na^+/H^+ exchange (as determined by pH_i and $^{22}Na^+$ influx measurements; Figures 4–7). Figure 4 shows that the recovery after β-alanine–induced intracellular acidification is slow in the absence of extracellular Na^+ and after addition of Na^+ to the basal solution, but is dependent on readdition of Na^+ to the apical superfusate. Similar observations have been made with the dipeptide Gly-Sar (26). (Note that the apical pH 5.5 solution and β-alanine were added together; previous experiments [5, 7] with both Gly-Sar and β-alanine demonstrate that the acidification is due to the presence of substrate and not apical acidity alone.) A comparison of the mean H^+ efflux rates (Figure 5) after acidification demonstrates that the pattern of stimulation of Na^+-dependent or -independent efflux differs depending on the method of acidification. NH_4Cl activates Na^+-dependent H^+ efflux across both membranes, whereas solute activates a large Na^+-dependent H^+ efflux at the apical surface, with only a marginal stimulation (yet greater than in the absence of Na^+) at the basolateral membrane. Figure 6 demonstrates that even in conditions where the ability of EIPA to inhibit Na^+/H^+ exchange is reduced (at 137 mM Na^+), recovery after solute-induced acidification by either β-alanine or Gly-Sar is reduced in the presence of 100 μM EIPA. $^{22}Na^+$ influx experiments (Figure 7) confirm that after acidification induced by dipeptide or amino acid, there is a significant increase in Na^+ influx across the apical membrane ($P < 0.001$ for both solutes at pH 5.5 vs. pH 5.5 alone). This influx can be significantly inhibited by 100 μM EIPA, from 236.2 ± 9.7 ($n = 11$) to 64.9 ± 3.9 ($n = 12$) fmol•cm^{-2} using β-alanine ($P < 0.001$), and from 205.5 ± 10.2 ($n = 10$) to 65.8 ± 6.9 ($n = 12$) fmol•cm^{-2} using Gly-Sar ($P < 0.001$). There was no significant change in $^{22}Na^+$ influx across the basolateral membrane after incubation with either Gly-Sar or β-alanine ($P > 0.05$).

Discussion

The results of this study demonstrate the importance of functional coexpression of transport proteins (involved in both pH_i homeostasis and solute transport) to human intestinal absorption. The results are entirely consistent with the polarized expression of NHE isoforms in human intestinal epithelial (Caco-2) cell monolayers (Figure 3). The EIPA sensitivity (IC_{50}) of the apical and basolateral membrane Na^+/H^+ exchange activity is similar to that for cloned NHE3 and NHE1 (17), respectively, suggesting that NHE3 is localized at the apical membrane and NHE1 at the basolateral membrane. Because only a minor component of apical $^{22}Na^+$ influx is blocked at 1 μM EIPA, apical NHE2 activity must be low compared with NHE3 activity. A comparison of the Caco-2 NHE2 sequence with that from the human duodenum reveals that over the sequenced region, the amino acid sequence is 98% identical. However, we cannot exclude the possibility that the amino acid substitutions in the NHE2 sequence might lead to an inactivation or a change in NHE2 function (this has not been studied further). In the human intestine, Na^+/H^+ exchange activity has been demonstrated in jejunal brush border membrane vesicles (27). mRNA for the Na^+/H^+ exchangers NHE1, NHE2, and NHE3 is distributed throughout the human small intestine and colon (20). Immunohistochemical studies demonstrate that both human NHE2 and NHE3 are localized at the apical membrane of human intestinal tissues (28). Broadly speaking, under the cell culture conditions used in this study (high-density seeding; monolayers ≥ 14 days old), the distribution of Na^+/H^+ exchange in Caco-2 cells reflects observations made in human intestinal tissues. This is an important observation regarding the validity of this study, because the cells can be grown under other culture conditions where NHE3 activity is absent from the apical surface (23).

The H^+/dipeptide cotransporter PepT1 has been localized to the apical membrane of the human intestine and the Caco-2 cell (18). The results in Figures 4–7 demonstrate that both H^+-coupled dipeptide and amino acid symport at the apical membrane activate the apical, but not basolateral, Na^+/H^+ exchanger. A similar preferential activation of either apical or basolateral Na^+/H^+ exchange has been observed in HT29 human colonic epithelial cells after sustained exposure to short-chain fatty acids from the apical or basal

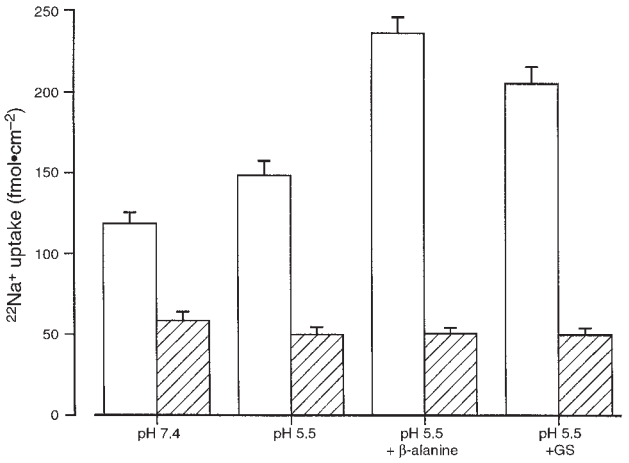

Figure 7
Solute-induced Na^+/H^+ exchange activity in Caco-2 cell monolayers. $^{22}Na^+$ influx across apical (open bars) and basolateral (hatched bars) membranes of Caco-2 cell monolayers. The monolayers were subjected to a 15-minute preincubation with the apical solutions indicated on the diagram; basal solution was pH 7.4 and contained 1 mM ouabain. Influx was performed at pH 7.4 for 5 minutes. Results are mean ± SEM (n = 10–12).

solutions (12). Because kinentic differences between NEH1 and NEH3 activation by a reduction in pH_i are not consistent (24, 29), and because NHE1 activation by a reduction in pH_i shows similar sensitivity to NHE2 and NHE3 activation in fetal bovine serum (24), the simplest explanation for these data is that the local pH in the cytosol adjacent to either the brush border or basolateral membrane may be the prime determinant in activating Na^+/H^+ exchange at either membrane. This raises the possibility that H^+/substrate cotransport localized to the apical brush border membrane will result in a pH at that site which is more acidic than most of the cytosol. This may preferentially activate brush border Na^+/H^+ exchange that optimizes transepithelial Na^+ absorption (apically by NHEs; basolaterally by Na^+,K^+-ATPase) without activating "futile" Na^+ cycling at the basolateral membrane (by basolateral NHEs and basolateral Na^+,K^+-ATPase) (12). The converse is also true, with maximal H^+/substrate cotransport being achieved only when apical Na^+/H^+ exchange is active. Thus H^+ will recycle across the apical membrane, maintaining both pH_i and an important driving force for solute absorption — the H^+ electrochemical gradient — with energy originating from Na^+,K^+-ATPase activity. These observations support studies in both turtle colon (30) and murine macrophages (31) that demonstrate that Na^+/H^+ exchange activity can generate local pH microdomains that stimulate activation of an H^+ conductance. Whether such activity would occur in vivo is unclear, but the observations in this study highlight the physiological relevance of such microdomains in a system where there is a strong possibility that these microdomains may be produced and maintained.

The local pH microclimate is likely to vary depending on the state of the pre- and postprandial lumen. Therefore, system parameters (transepithelial Na^+ transport) cannot be predicted simply by knowledge of the detailed kinetics and regulation of NHE isoforms. Optimization of system performance (Na^+ and solute absorption) requires that membrane transporters are colocalized within specialized membrane domains, and act in a linked and mutually dependent fashion. In NHE3-deficient mice, there is a severe absorptive defect in the intestine (32), with compensatory change observed in the colon that includes upregulation of H^+,K^+-ATPase activity and Na^+ channel density. Similar principles to those shown here for intestine may apply in other epithelia (e.g., the proximal tubule). A study using NHE3-deficient mice reveals that HCO_3^- and fluid reabsorption are sharply reduced in proximal convoluted tubule, due to lack of H^+ extrusion dependent on NHE3 activity (32).

The expression of multiple NHE isoforms within a single cell implies that additional features (e.g., regulation by protein kinases) other than domain localization are required for appropriate physiological activity. Whereas apical Na^+/H^+ exchange driven by local pH change may optimize absorptive function, basolateral Na^+/H^+ exchange may be primarily a homeostatic mechanism controlling bulk cytosolic pH and cell volume.

Acknowledgments

This study was supported by the Biotechnology and Biological Sciences Research Council and the Wellcome Trust. Technical support was provided by Charlotte Ward and Maxine Geggie.

1. Daniel, H. 1996. Function and molecular structure of brush-border membrane peptide/H^+ symporters. *J. Membr. Biol.* **154**:197–203.
2. Leibach, F.H., and Ganapathy, V. 1996. Peptide transporters in the intestine and the kidney. *Annu. Rev. Nutr.* **16**:99–119.
3. Hoshi, T., Takuwa, N., Abe, M., and Tajima, A. 1986. Hydrogen ion-coupled transport of D-glucose by phlorizin-sensitive sugar carrier in intestinal brush-border membranes. *Biochim. Biophys. Acta* . **861**:483–488.
4. Hirayama, B.A., Loo, D.D.F., and Wright, E.M. 1994. Protons drive sugar transport through the Na^+/glucose cotransporter (SGLT1). *J. Biol. Chem.* **269**:21407–21410.
5. Thwaites, D.T., Brown, C.D.A., Hirst, B.H., and Simmons, N.L. 1993. Transepithelial glycylsarcosine transport in intestinal Caco-2 cells mediated by expression of H^+-coupled carriers at both apical and basal membranes. *J. Biol. Chem.* **268**:7640–7642.
6. Thwaites, D.T., Cavet, M., Hirst, B.H., and Simmons, N.L. 1995. Angiotensin-converting enzyme (ACE) inhibitor transport in human intestinal epithelial (Caco-2) cells. *Br. J. Pharmacol.* **114**:981–986.
7. Thwaites, D.T., McEwan, G.T.A., Brown, C.D.A., Hirst, B.H., and Simmons, N.L. 1993. Na^+-independent, H^+-coupled transepithelial β-alanine absorption by human intestinal Caco-2 cell monolayers. *J. Biol. Chem.* **268**:18438–18441.
8. Thwaites, D.T., Armstrong, G., Hirst, B.H., and Simmons, N.L. 1995. D-cycloserine transport in human intestinal epithelial (Caco-2) cells is mediated by a H^+-coupled amino acid transporter. *Br. J. Pharmacol.* **115**:761–766.
9. McEwan, G.T.A., Daniel, H., Fett, C., Burgess, M.N., and Lucas, M.L. 1988. The effect of *Escherichia coli* STa enterotoxin and other secretagogues on mucosal surface pH of rat small intestine in vivo. *Proc. R. Soc. Lond. B.* **234**:219–237.
10. Rawlings, J.M., Lucas, M.L., and Russel, R.I. 1987. Measurement of jejunal surface pH in situ by plastic pH electrode in patients with coeliac disease. *Scand. J. Gastroenterol.* **22**:377–384.
11. Chu, S., and Montrose, M.H. 1995. Extracellular pH regulation in microdomains of colonic crypts: effects of short-chain fatty acids. *Proc. Natl. Acad. Sci. USA.* **92**:3303–3307.
12. Rowe, W.A., Lesho, M.J., and Montrose, M.H. 1994. Polarized Na^+/H^+

exchange function is pliable in response to transepithelial gradients of propionate. *Proc. Natl. Acad. Sci. USA.* **91**:6166–6170.
13. Thwaites, D.T., McEwan, G.T.A., and Simmons, N.L. 1995. The role of the proton electrochemical gradient in the transepithelial absorption of amino acids by human intestinal Caco-2 cell monolayers. *J. Membr. Biol.* **15**:245–256.
14. Aronson, P., Nee, J., and Suhm, M.A. 1982. Modifier role of internal H^+ in activating the Na^+/H^+ exchanger in renal microvillus membrane vesicles. *Nature* . **299**:161–163.
15. Murer, H., Hopfer, U., and Kinne, R. 1976. Sodium/proton antiport in brush-border-membrane vesicles isolated from rat small intestine and kidney. *Biochem. J.* **154**:597–604.
16. Orlowski, J., and Grinstein, J. 1997. Na^+/H^+ exchangers of mammalian cells. *J. Biol. Chem.* **272**:22373–22376.
17. Noel, J., and Pouyssegur, J. 1995. Hormonal regulation, pharmacology, and membrane sorting of vertebrate Na^+/H^+ exchanger isoforms. *Am. J. Physiol.* **268**:C283–C296.
18. Maher, M.M., Gontarek, J.D., Bess, R.S., Donowitz, M., and Yeo, C.J. 1997. The Na^+/H^+ exchange isoform NHE3 regulates basal canine ileal Na^+ absorption in vivo. *Gastroenterology*. **112**:174–183.
19. Walker, D., Thwaites, D.T., Simmons, N.L., Gilbert, H.J., and Hirst, B.H. 1998. Substrate up-regulation of the human small intestinal peptide transporter, hPepT1. *J. Physiol.* **507**:697–706.
20. Dudeja, P.K., et al. 1996. Intestinal distribution of human Na^+/H^+ exchanger isoforms NHE-1, NHE-2, and NHE-3 mRNA. *Am. J. Physiol.* **271**:G483–G493.
21. Brant, S.R., Yun, C.H.C., Donowitz, M., and Tse, C.M. 1995. Cloning, tissue distribution, and functional analysis of the human Na^+/H^+ exchanger isoform, NHE3. *Am. J. Physiol.* **269**:C198–C206.
22. Ghishan, F.K., Knobel, S.M., and Summar, M. 1995. Molecular cloning, sequencing, chromosomal localization, and tissue distribution of the human Na^+/H^+ exchanger (SLC9A2). *Genomics*. **30**:25–30.
23. Watson, A.J.M., Levine, S., Donowitz, M., and Montrose, M.H. 1991. Kinetics and regulation of a polarized Na^+-H^+ exchanger from Caco-2 cells, a human intestinal cell line. *Am. J. Physiol.* **261**:G229–G238.
24. Levine, S.A., Montrose, M.H., Tse, C.M., and Donowitz, M. 1993. Kinetics and regulation of three cloned mammalian Na^+/H^+ exchangers stably expressed in a fibroblast cell line. *J. Biol. Chem.* **268**:25527–25535.
25. Sardet, C., Counillon, L., Franchi, A., and Pouyssegur, J. 1989. Molecular cloning, primary structure, and expression of the human growth factor-activatable Na^+/H^+ antiporter. *Cell* . **56**:271–280.
26. Thwaites, D.T., Hirst, B.H., and Simmons, N.L. 1994. Substrate specificity of the di/tripeptide transporter in human intestinal epithelia (Caco-2): identification of substrates that undergo H^+-coupled absorption. *Br. J. Pharmacol.* **113**:1050–1056.
27. Kleinman, J.G., Harig, J.M., Barry, J.A., and Ramaswamy, K. 1995. Na^+ and H^+ transport in human jejunal brush-border membrane vesicles. *Am. J. Physiol.* **255**:G206–G211.
28. Hoogerwerf, W.A., et al. 1996. NHE2 and NHE3 are human and rabbit intestinal brush-border proteins. *Am. J. Physiol.* **270**:G29–G41.
29. Orlowski, J. 1993. Heterologous expression and functional properties of amiloride high affinity (NHE-1) and low affinity (NHE-3) isoforms of the rat Na/H exchanger. *J. Biol. Chem.* **268**:16369–16377.
30. Post, M.A., and Dawson, D.C. 1994. Basolateral Na^+-H^+ exchanger. *J. Gen. Physiol.* **103**:895–916.
31. Demaurex, N., Orlowski, J., Brisseau, G., Woodside, M., and Grinstein, S. 1995. The mammalian Na^+/H^+ antiporters NHE-1, NHE-2, and NHE-3 are electroneutral and voltage independent, but can couple to an H^+ conductance. *J. Gen. Physiol.* **106**:85–111.
32. Schulthesis, P.J., et al. 1998. Renal and intestinal absorptive defects in mice lacking the NHE3 Na^+/H^+ exchanger. *Nat. Genet.* **19**:282–285.